Polymer Degradation and Stability 94 (2009) 1639–1645

Contents lists available at ScienceDirect

Polymer Degradation and Stability

journal homepage: www.elsevier.com/locate/polydegstab

The use of SSA fractionation to detect changes in the molecular structure of model ethylene–butene copolymers modified by peroxide crosslinking

Claudio J. Pérez [a,*], N. Villarreal [b], J.M. Pastor [b,c], M.D. Failla [d], E.M. Vallés [d], J.M. Carella [a]

[a] Instituto de Investigaciones en Ciencia y Tecnología de Materiales (INTEMA) (UNMdP-CONICET), Facultad de Ingeniería, Universidad Nacional de Mar del Plata, Juan B. Justo 4302, 7600 Mar del Plata, Argentina
[b] CIDAUT, Foundation for Research and Development in Transport and Energy, Parque Tecnológico de Boecillo P. 209, 47151 Boecillo, Valladolid, Spain
[c] Departamento de Física de la Materia Condensada, E.T.S.I.I., Universidad de Valladolid, 47011 Valladolid. Spain
[d] Planta Piloto de Ingeniería Química-PLAPIQUI (UNS-CONICET), Camino "La Carrindanga" Km 7, 8000 Bahía Blanca, Argentina

ARTICLE INFO

Article history:
Received 5 May 2009
Received in revised form
22 June 2009
Accepted 7 July 2009
Available online 14 July 2009

Keywords:
Ethylene–butene copolymers
Organic peroxide
Crosslinking
Successive self-nucleation and annealing

ABSTRACT

Four model ethylene–butene copolymers of different molecular weights modified with various concentrations of peroxide were analyzed by a DSC based successive self annealing method. The original copolymers had the same intra and intermolecular homogeneous branching distribution along the linear chains with approximately 2.4% mol of ethyl branches. The copolymers with average molecular weights of 29,000, 45,000, 81,000 and 125,000 g/mol were modified with different amounts of 2,5-dimethyl-2,5-di(tert-butyl peroxy)-hexane (DBPH) as a crosslinking initiator. The molecular changes induced by the reaction with the peroxide affect the semicrystalline structure of the material. Variations in the crystal thickness distributions of the material as a consequence of the modification are related to the peroxide induced free radical reactions.

1. Introduction

The modification of poly(ethylene) (PE) by post-reactor processes is used to generate materials with specific properties, different from those of the original material and potentially useful in different applications [1–3]. Crosslinking is one of the most widely employed modification methods available to increase the range of thermal resistance of this polymer and several of its copolymers. This reaction can be conducted via free radicals obtained by decomposition of chemical agents or by physical methods such the decomposition of organic peroxides or diazocarbamides, or by ionizing radiation from several types of sources [4–8]. One of the advantages of peroxide modification is that it may be carried out with normal processing equipment, without much requirement for special installations.

The most important reactions that occur during the polymer modification process by free radicals are those that induce links between activated macroradicals generating long branches and elastically active chains. Depending on the nature of the original polymer and on the conditions of the modification reaction chain scission may be also present at various levels. These reactions contribute to reduce the molecular weight of the polymer inducing additional changes on the molecular structure [9,10]. With the development of the modification process, the average molecular structure of the original PE chains changes. Chains that undergo crosslinking have their average molecular weights increased via long-chain branching, and the molecular weight distribution of the polymer becomes wider. Chains that undergo scission contribute mostly to enlarge the lower end of the molecular weight distribution [4–20]. At large extents of the modification process a molecular network forms giving origin to a gel structure that is no longer soluble.

The Successive Self-nucleation and Annealing (SSA) technique has been developed to characterize semicrystalline polymers that are capable of forming families of lamellae with different average thickness at controlled cooling stages [21–24]. Fractionation during crystallization can be induced in polymers because of differences in chain branching frequency. The fundamental reason behind fractionation is the dependence of crystallization temperature on the uninterrupted length of the crystallizable polymethylene chain segments. Crosslinking interrupts the linear polymethylene sequences, thus preventing the formation of thicker lamellae, and changing the SSA spectra as the modification

* Corresponding author.
E-mail address: cjperez@fi.mdp.edu.ar (C.J. Pérez).

0141-3910/$ – see front matter © 2009 Elsevier Ltd. All rights reserved.
doi:10.1016/j.polymdegradstab.2009.07.002

reaction advances [23]. Regular DSC is used to thermally conditioning the samples and to record the output from the final heating run, from which the effects of fractionation can be analyzed. The SSA technique can render results similar to those obtained by Temperature Rising Fractionation (TREF) or by Crystallization Analysis Fractionation (CRYSTAF), without the need to fully solubilize the polymers; thus, SSA can be used for crosslinked polymers past the gel point.

In the present work, we study the molecular structure changes of hydrogenated polybutadienes obtained by anionic polymerization. The original polymers have narrow molecular mass distribution and very narrow and homogeneous chains branching frequency distribution, which are chemically analog to linear ethylene–(butene-1) copolymers. These polymers were modified using DBPH peroxide as initiator to obtain a crosslinked material. The original and the modified polymers, below and above the gel point, were analyzed using an SSA thermal treatment. The observed crystallite thickness distribution changes are discussed and used to complement previous results where the evolution of the molecular structure of the modified polymers was studied by following the changes on the molecular weight distribution by gel permeation chromatography and low angle laser light scattering.

2. Experimental

2.1. Materials

Linear polybutadienes (PB) were synthesized by anionic polymerization of butadiene following standard methods in cyclohexane solution [24–26]. Infrared spectroscopy (IR) was used to determine the microstructure of the PB's, using a Nicolet 520 FT-IR spectrometer. 9–10% of the butadiene units were polymerized following a 1,2-addition path.

Polybutadienes were hydrogenated in toluene solution using a Wilkinson's catalyst ($RhCl(PPh_3)_3$), purchased from Strem Chemicals Inc. Hydrogenation was performed at 90 °C on a Parr reactor, at 700 psi of hydrogen pressure [27]. HPBs chemical structure strictly consists of polymethylene sequences connected by tertiary carbon atoms that contain ethyl branches, with about 24 CH_3/1000 C. Due to the polybutadiene homopolymerization procedure, polymethylene lengths distributions are truly random.

To evaluate the possible presence of residual unsaturations, infrared spectra of the hydrogenated polybutadienes were recorded on 0.1 mm thick films monitoring the absorption peaks at 910 cm^{-1} and 966 cm^{-1} (vinyl and trans isomers). No double bonds were found on the samples used for this work.

The changes on the molecular weight distributions of the hydrogenated polymers was followed by Size Exclusion Chromatography (SEC) on a Waters 150-C ALP/GPC operating at 135 °C, using 1,2,4 trichlorobenzene as solvent. The chromatograph was equipped with a refractive index detector and with on-line Multi Angle Light Scattering detector (MALS) from Wyatt Technology (Dawn DSP). Table 1 lists the properties of the four polymers used in this study. The denomination adopted for these materials is of the form HPB#, where # is the number that identifies the average molecular weight of the polymer.

Table 1
Average molecular weights (g/mol) of the original and modified HPB's estimated from MALLS–SEC, fraction gel (%), crosslinked fractions, Fusion enthalpy (kJ/kg), Crystallization and Melting temperature (°C) values obtained from Fig. 2.obtained during the modification.

Polymer	Peroxide (wt%)	Mw × 10^{-3} (g/mol)	Gel (%)	T_c (°C)	T_m(°C)	Fusion enthalpy (kJ/kg)
HPB-29	0.00	29 ± 1	–	97.5	110.3	128.6
	0.30	44 ± 3	0	95.2	109.8	126.6
	0.50	55 ± 4	0	93.6	109.5	125.1
	1.00	167 ± 10	24 ± 3	90	107.8	123.3
	5.00	23 ± 3	90 ± 3	79	105.4	115.7
HPB-45	0.00	45 ± 2	–	94	109.5	123.3
	0.20	50 ± 5	0	94	109	117.8
	0.40	63 ± 4	0	93.6	109.4	114.3
	0.50	106 ± 10	5 ± 2	92.5	108.5	111.3
	1.00	308 ± 21	33 ± 3	87.9	109.4	110.5
HPB-81	0.0	81 ± 3	–	93.1	108	116.0
	0.05	89 ± 7	0	91.7	107.6	114.3
	0.10	94 ± 8	0	92.1	107.4	112.2
	0.20	186 ± 10	0	89.6	106.7	110.7
	1.00	189 ± 11	76 ± 3	85.6	105.1	97.9
	2.00	91 ± 8	88 ± 5	78.9	99.2	93.8
HPB-125	0.00	125 ± 5	–	91.1	109.3	122.2
	0.05	149 ± 4	0	92.4	108.2	121.6
	0.10	165 ± 3	0	91.6	108.3	119.0
	0.20	366 ± 16	50 ± 4	89.8	108.6	114.3
	0.50	265 ± 7	76 ± 6	87.4	108.9	112.8
	1.00	215 ± 10	88 ± 4	86.4	106.4	109.6

2.2. Modification procedure

2,5-dimethyl-2,5-di(tert-butyl peroxy)-hexane (DBPH) (Akzo Chemical of Argentina) was used as initiator of the modification process. HPBs in the form of fine powder were impregnated with different amounts of a peroxide-hexane solution. Afterwards, the solvent was evaporated inside a hood. This method provides a homogeneous dispersion of the peroxide on the polymer [5,14,15], with concentrations ranging from 0.05 to 5.00% w/w based on the polymer.

Impregnated HPBs were then placed between 3 mm thick steel plates lined with aluminum foils, held apart by a 1 mm thick aluminum frame. Finally, the samples were compression molded between the hot plates of a hydraulic press for 30 min at 170 °C. The reaction time necessary to complete the reaction was estimated by performing rheological tests following the method utilized by Bremner et al. [15] for monitoring curing reactions.

The gel fraction was determined by extracting the soluble portion of different specimens of each modified polymer with xylene at 125 °C.

2.3. Evaluation of basic thermal behavior

Whole (not extracted) samples were used throughout for all DSC characterization and SSA. Small disc samples (approximately 10 mg) were cut from films of all original and modified HPBs. The samples were encapsulated in DSC aluminum pans and ultra high purity dry nitrogen was used as an inert atmosphere for conditioning and tests in a Mettler Toledo DSC 821/700 calorimeter. A first characterization of the thermal behavior of the polymers was performed on the DSC by cooling and heating runs between 25 and 200 °C at a heating rate of 10 °C/min. In order to erase all previous thermal history all the samples were previously held in the molten state at 150 °C for 5 min.

2.4. SSA technique

The SSA technique consists of successive heating and cooling cycles. The self-nucleation and annealing temperatures (T_{si}) were chosen according to a regime defined by Fillon et al. [28]. Samples were heated and held at 150 °C for 5 min. Afterwards, they were cooled down to 40 °C at 10 °C/min to give an initial

standard thermal history. Another heating scan followed, at the same rate, to a selected self-seeding temperature denoted T_s, then kept for 5 min at that temperature before cooling it again down to 40 °C at the same rate. The first applied T_s is chosen so that the polymer will only self-nucleate (i.e. T_s would be high enough to melt all the crystalline regions, except for small crystals fragments and/or nuclei that can later self-seed the polymer during cooling (around 120–122 °C)). After that, the samples were heated once again up to a temperature 5–6 °C below T_s and held for 5 min. The crystals not melted at this temperature would anneal and some of the molten species would isothermally crystallize at this new temperature. The remaining molten crystallizable chains would only crystallize during the subsequent cooling. This cyclic procedure was repeated by heating the sample at a temperature 5–6 °C lower than that of the previous annealing, until a heating temperature close to 40 °C was reached. Melting patterns of the samples thus prepared were recorded at a heating rate of 10 °C/min. The final heating scan after this thermal fractionation reveals a series of multiple melting peaks (as shown in Fig. 3) that are a reflection of the multiple mean lamellar thicknesses obtained. The general procedure is similar to that represented in Fig. 1 and the conditions used for the SSA are shown on in parenthesis in the first column of Table 2.

3. Results and discussion

Four HPBs were used for this study, with average molecular weights ranging from 29,000 to 125,000 g/mol. The modification of the HPBs with the peroxide DBPH is assumed to progress according to the general crosslinking and scission reactions scheme proposed for the free radical mechanism [4,5].

The evolution of the number and weight average molecular weights of the polymers modified with increasing peroxide concentrations are reported on Table 1. In order to estimate the relative rates of the scission and crosslinking that results from the modification process, the mass fractions of polymer chains with molecular weights higher and lower than the original polymers was calculated from the areas of the MALS–SEC traces. This was done for all those polymers modified with peroxide concentrations lower than those necessary to reach the gel point [9]. The scission process produces a fraction of molecules with molecular weights lower than the corresponding to the original polymer that amounts between 3 and 5%. This fraction is very similar to the observed when similar HPB are modified by high ionizing radiation [10].

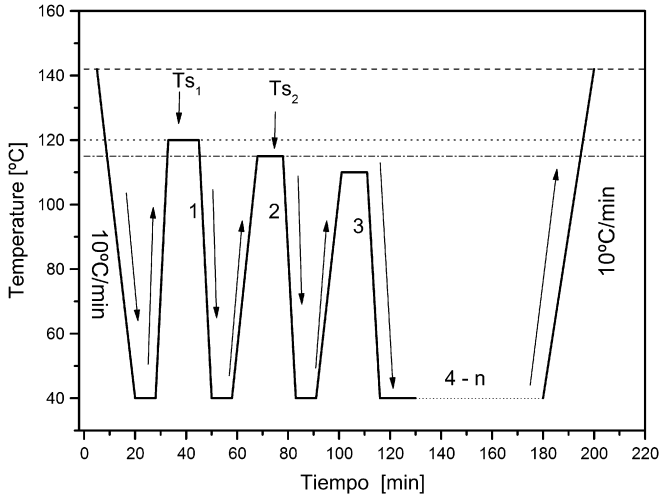

Fig. 1. General description of the SSA technique steps.

Table 1 also reports the fraction of gel-expressed as percentage of total mass-that was obtained for each of the HPBs modified with peroxide concentrations beyond those necessary to reach the critical gel dose. These results show that for this system the critical dose required to reach the gel point depends on the original molecular weight of the different HPBs as predicted by theory [29].

As an example of the general trend observed for the thermal behavior of all the modified HPBs, the usual DSC traces for the crystallization process of the original HPB-81 polymer and those that correspond to the same material modified with different amounts of DBPH are shown in Fig. 2a and b shows the corresponding melting DSC outputs. For this HPB-81, 2.00 wt% DBPH produces about 80% gel that remains semicrystalline. The formation of crosslinked junctions and the chain scissions induced by the modification process change the length distribution of the crystallizable regular polymethylene chains segments placed between neighboring tertiary carbons that belong to branching or crosslinking points. These changes alter the final lamellae thickness distribution during crystallization. Consequently the melting and crystallization temperatures are modified by the peroxidation reaction.

The thermal properties for all the original and modified HPBs polymers: melting temperature peak (T_m), crystallization temperature peak (T_c) and heat of fusion (ΔH) are reported on Table 1. For all modified samples, increasing peroxide concentrations cause reductions on T_c and T_m, as well as on the enthalpy of fusion. Crosslink points play two main roles on the changes observed on the thermal properties. First, they act as defect centers since they are not included in crystalline registry. Second, the observed raise on the molecular weight as well as the topological restrictions caused by crosslink points may also difficult some of the macromolecular chains short-range transport

Table 2
Melting peak temperatures for all melting endotherms obtained after the SSA treatment (Figs. 3a–3d) as a function of self-seeding temperature (T_s) and peroxide concentration.

Material (T_s range)	T_m (°C)					
HPB-29 (117–62 °C)	T_s (°C)	Concentration of peroxide (wt%)				
		0.00	0.30	0.50	1.00	5.00
	111	111.3	110.5	109.7	–	–
	105	105.6	106.8	104.8	108	–
	99	100.7	101.2	100.4	101.8	102.9
	93	95.8	96.3	95.6	96.6	98.6
	87	90.8	91.2	90.8	91.6	93
HPB-45 (118–52 °C)		0.00	0.20	0.40	0.50	1.00
	112	111.4	111	110.4	111.9	–
	106	105.2	105.3	104.5	106.1	108.5
	100	99.1	99	98.4	99.3	100.4
	94	92.9	92.8	92.6	93.1	94
	88	86.9	86.8	86.5	87.2	88
HPB-81 (116–55 °C)		0.00	0.05	0.10	0.20	1.00	2.00
	110	110.6	110.3	110.4	–	–	–
	105	105.4	105.3	105.2	106.4	107.1	–
	100	100.1	99.9	100	100.4	101.6	100.4
	95	94.7	94.8	94.9	94.9	95.7	95.9
	90	89.6	89.7	89.7	89.9	90.6	90.2
HPB-125 (125–59 °C)		0.00	0.05	0.10	0.20	0.50	1.00
	107	107.9	107.8	108.6	109.1	109.4	108.1
	101	100.7	100.8	100.9	101.2	102.4	102.6
	95	94.4	94.3	94.4	94.6	95.6	95.1
	89	88.2	88	88.2	88.6	89.4	89.1

movements needed for the crystallization stage evolution to occur. Both effects may decrease the crystal lamellar thickness and the total amount of crystallizable linear polymethylene sequences. Distributions of melting temperatures obtained by DSC, as shown in Fig. 2, can be used to roughly estimate lamellar thickness distributions. Employing this procedure the results are not completely reliable, as crystallization at a finite cooling rate may not be complete due to topological restrictions, and melting in the presence of liquid HPB somewhat reduces the measured melting temperature [30]. From this point of view, SSA results are much better and precise since the self annealing stage minimizes the mobility restriction effect of crosslink points acting as topological obstacles.

Fig. 3a–d present the final melting runs after applying the SSA technique to the materials under study. The SSA treatment applied allows separation of between six and seven populations of lamellae in the same thickness range in every sample. Each DSC peak corresponds to the melting of crystallites with different average thickness, which increases with melting temperature. Only those temperature values capable of producing self-nucleation and annealing are reported in Table 2 (T_s), since they are directly responsible for the annealed crystals that subsequently melt during the final heating. The melting points (T_m) of all the populations produced per sample are shown in the same table.

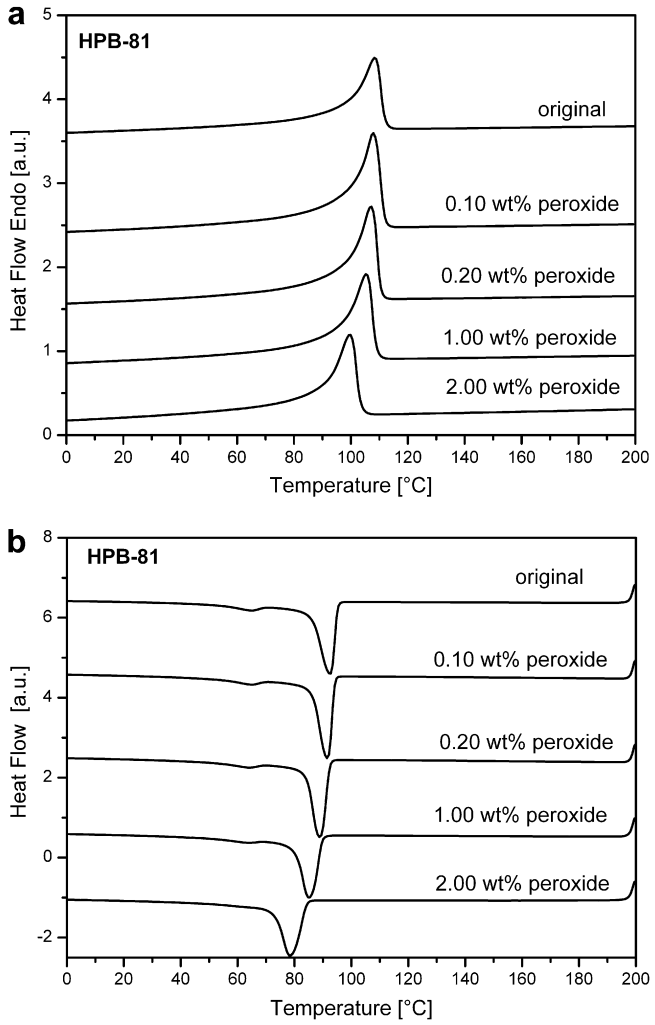

Fig. 2. DSC heating (a) and cooling (b) scans at 10 °C/min for the original HPB-81 and the modified polymers obtained.

Final melting peaks after SSA treatment, that reflects narrow distributions of lamellae thicknesses, will depend on the crystallizable polymethylene lengths available, and also on the set of T_s temperatures chosen. The T_s set was kept to be almost the same for all samples, to study true evolution of amounts of particular crystallizable polymethylene sequences. As final melting maximum temperature values change for peroxide treated samples, the evolution of the peaks corresponding to the maxima on untreated samples was followed by deconvoluting all DSC final melting curves. Untreated samples rendered single deconvoluted peaks, and peroxide treated samples were deconvoluted with the condition of finding true peaks centered at the same maxima as found for untreated samples. Fig. 4 depicts typical results for HPB-81 treated with 1.00 wt% peroxide. The partial areas corresponding to each of the deconvoluted peaks are tabulated in Table 3. For example the areas obtained from the deconvolution performed on Fig. 4 are reported in the column identified as 1.00 in the row corresponding to HPB-81. The original endotherm N° 2, centered at 105.4 °C for the original HPB-81 is now decomposed in 2 peaks, with one of them centered at 105.4 °C. Main discussion is centered on these peaks evolution.

Table 3 shows the area fractions for the crystallite thicknesses corresponding to each of the endothermic peaks found for the original HPB, and reported on Fig. 3a–d. Areas under those peaks were calculated from deconvolution of the SSA–DSC outputs shown in Fig. 3a–d for the peroxide treated samples. Areas reported in Table 3 correspond to the deconvoluted peaks centered at the peaks of the SSA–DSC trace for the original polymer. In the case of the original HPBs samples, as the polymers used have very similar distributions of crystallizable chain lengths, the small peak temperature shifts at the high temperature side of the SSA–DSC trace are assumed to follow the small differences in the T_s temperatures used for each sample.

The SSA–DSC endotherm areas are proportional to the mass fractions of crystalline phase that are formed at each self-seeding temperature T_s. The effect of a homogeneous modification reaction on secondary carbons ought to be proportional to the mass of available crystallizable regular polymethylene chains segments, and thus associated changes in area fractions ought to be also proportional to the original area. As already mentioned above, crosslinking on methylene carbons is expected to reduce the lamellae thickness that can accommodate the resulting polymethylene shorter sequences. As the longest crystallizable polymethylene sequences that form the thicker lamellae are the most rapidly affected by the peroxide action, peroxide treated samples show early changes in lamellae thickness populations associated with the higher melting temperatures [31]. Chain scission at methyne carbon atoms is expected to produce pendant polymethylene chains ends with at least one topological restriction released, which may thus crystallize in lamellae thicker than the original ones.

Another fact to be taken into account is that available samples with different starting molecular weights have been treated with different amounts of peroxide, because the original main focus was the gel-forming effectiveness (a scale in the order of the molecular contour length), and here we need to compare the effect of peroxide attack on SSA–DSC traces (a scale about two orders of magnitude smaller) at gel-forming stages that are different for every sample. As an example, SSA–DSC traces for sample HPB-29 shows large changes for 0.30 wt% peroxide, and we need to compare it with sample HPB-45 treated with 0.20 wt% and 0.40 wt% peroxide; differences of peroxide concentration are in the order of 50%. Therefore, we focus our analysis mainly on comparing those samples treated with similar peroxide concentration.

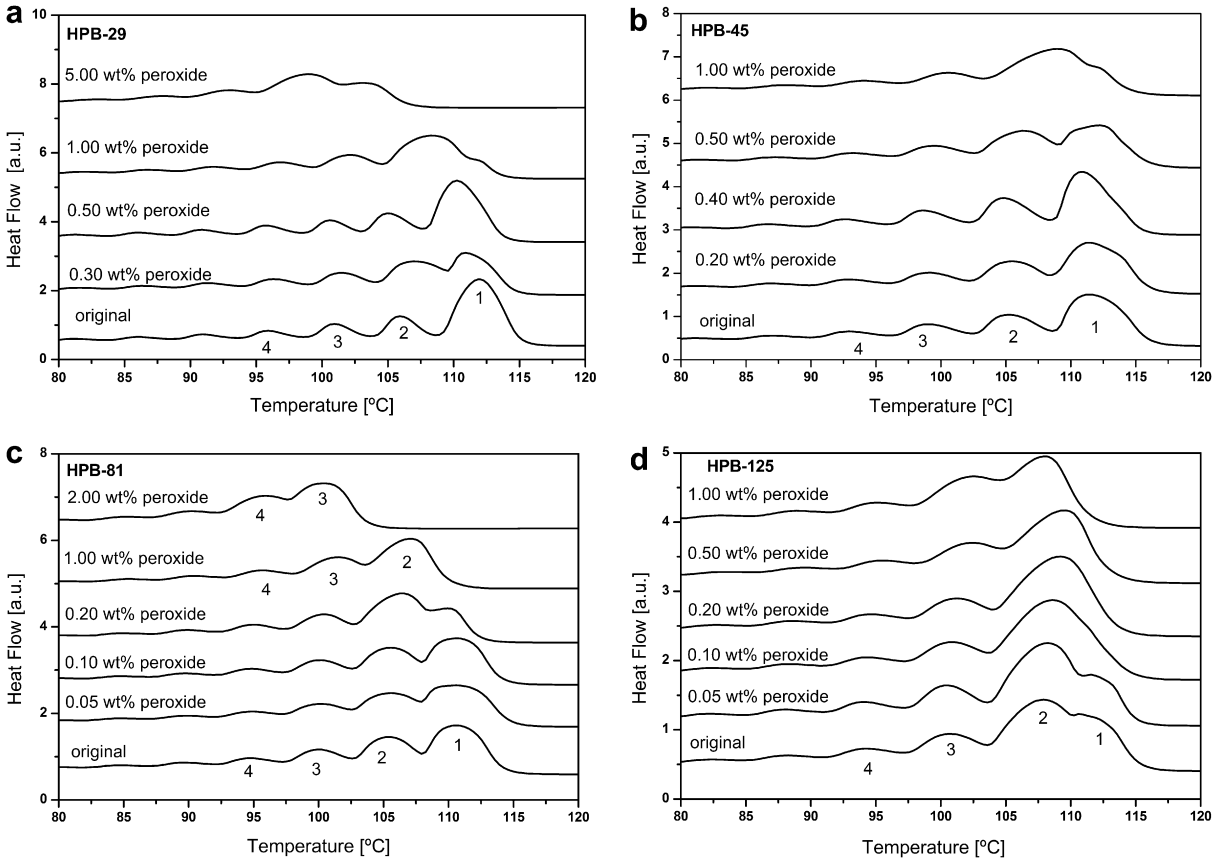

Fig. 3. Final DSC heating scans of an original and modified HPB-29 (a), original and modified HPB-45 (b), original and modified HPB-81(c) and original and modified HPB-125 (d). Heating proceeded at 10 °C/min, starting from 40 °C after applying Successive Self-nucleation/annealing (SSA).

For modified HPB-29 samples, a peak broadening and a height decrease are observed in the endotherm marked as 1 for the sample modified with 0.3 wt% peroxide, as compared with the original HPB-29 sample. For HPB-45 samples crosslinked with 0.20 wt% and 0.40 wt% of peroxide, some broadening is also observed in the endotherm marked as 1. For the HPB-45 samples

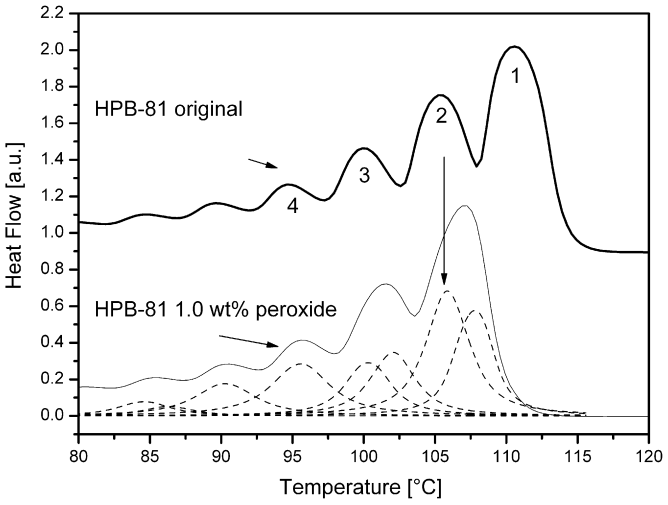

Fig. 4. Final DSC heating scans for original HPB-81, and for HPB-81 modified with 1.00 wt% peroxide. Dotted curves show deconvolution results for sample HPB-81 modified with 1.00 wt% peroxide. Data for peak 2 is used for analysis.

Table 3
Partial areas (%) for each DSC scan in Fig. 3a–d (i.e. after SSA) as a function of self-seeding temperature (T_s) and peroxide concentration.

Material	Partial area (%)						
HPB-29	T_s (°C)	Concentration of peroxide (wt%)					
		0.00	0.30	0.50	1.00	5.00	
	111	41.5	9.9	4.9	3.5	–	
	105	14.0	11.2	5.0	17.7	–	
	99	11.5	14.2	11.2	3.9	9.6	
	93	8.4	9.2	9	12.5	16.6	
	87	6.7	6.9	5.8	7.8	7.9	
HPB-45		0.00	0.20	0.40	0.50	1.00	
	112	37.0	38.9	35.9	15.2	6.2-	
	106	16.6	19.4	18.4	8.7	15.2	
	100	14.5	14.2	9.0	13.3	2.4	
	94	8.3	8.7	7.3	6.0	6.2	
	88	7.0	6.8	4.5	3.1	1.5	
HPB-81		0.00	0.05	0.10	0.20	1.00	2.00
	110	29	32.8	29.2	20.2-	–	–
	105	18.1	19.3	19.8	16	23	–
	100	12.4	12.7	13.1	35.8	10.2	26
	95	7.1	9.7	8.8	11.5	13.3	22.5
	90	3.7	5.2	5.7	6.2	8.5	12.3
HPB-125		0.00	0.05	0.10	0.20	0.50	1.00
	113	12.9	7.6	5.0	–	–	–
	107	36.5	44.9	44.0	55.5	27.6	27
	101	12.9	13.8	9.4	17.0	10.6	36.4
	95	9.9	9.9	10.2	9.1	5.5	10.0
	89	4.5	4.4	5.3	4.9	8.6	8.8

modified with 0.50 wt% and 1.00 wt% peroxide, an appreciable change is observed, as high temperature endotherms are almost eliminated. Similar effects can be observed for all samples used for this work.

For all samples, the elimination of the highest temperature SSA–DSC endotherms roughly coincides with the sudden appearance of gel as the critical dose of peroxide to reach the gel point in each of the polymers is surpassed. The fact that the highest temperature endotherm is eliminated at widely different peroxide doses for polymers with very similar branching distribution indicates that physical hindrance caused by the introduction of long chains and crosslinks on the polymer structure is not the main cause for this. These data rather points towards the influence of the medium-range chain translation processes on the chain folding needed for the crystallization process, which may be reduced for chains tightly packed in the melt, as is the case for polymers with high contour length concentration like polyethylene [32]. The presence of gel in the structure further reduces the reptation-like mobility of chains at the annealing stage of the SSA process, thus reducing the formation of the thicker lamellae.

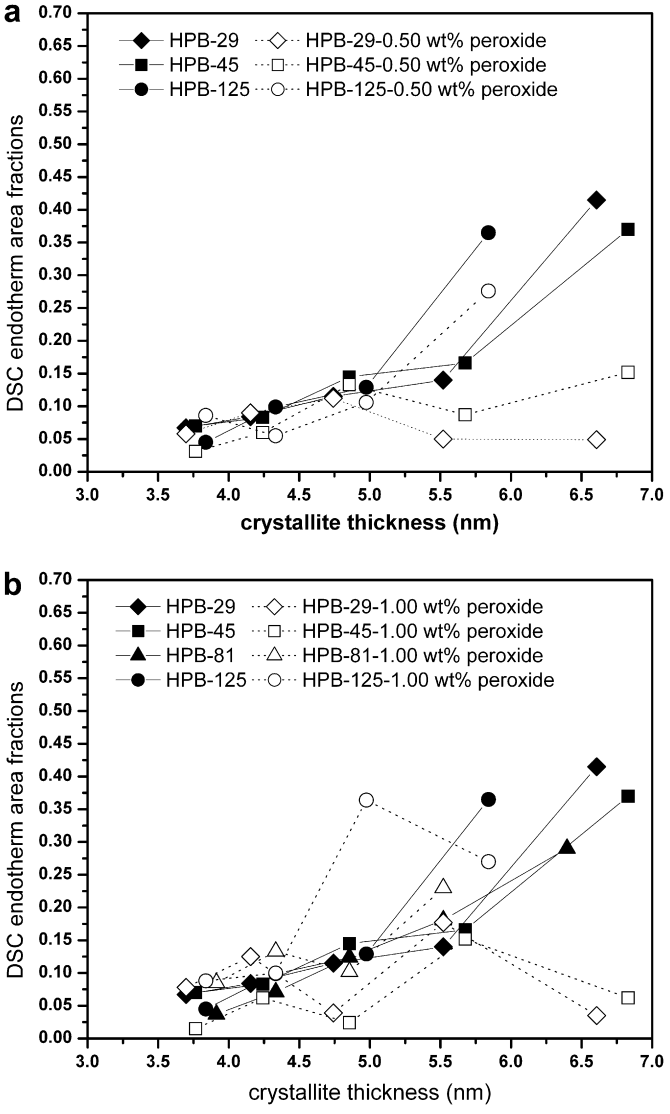

Fig. 5. Area fractions vs. lamellar thickness for original HPBs and modified with 0.50 wt% peroxide (a). Area fractions vs. lamellar thickness for original HPBs and modified with 1.00 wt% peroxide (b).

Polymethylene chains lengths forming the crystals that melt at the highest temperatures contain at least 60 carbon atoms, 1.5 times the average polymethylene sequence lengths for these polymers, and amount to only 2.3% of all polymethylene sequences [33]. Thus, small restrictions to the chain reptation at the annealing stage can prevent this small number of sequences to form crystals. Elimination of the higher temperature SSA–DSC endotherms is followed by an increase of the peak height of the lower temperature neighboring endotherm, and this process must be associated with shorter methylene sequences that become available for crystallization, or longest methylene sequences that can no reptate far enough for crystallization in thicker lamellae. For higher peroxide contents, lamellae that melt at the higher temperatures are successively eliminated, due to the same effects mentioned above.

The final heating run after an SSA treatment exhibits a series of melting peaks that correspond to the number of SSA cycles where annealing was promoted. Thompson-Gibbs equation [34] was used to calculate crystallite thickness from melting temperature:

$$I = \frac{2\sigma T_m^0}{\Delta H_v \left(T_m^0 - T_m\right)} \tag{1}$$

The values reported by Starck [34] were assumed to be constant: lamellar surface free energy (σ: 0.07 J m^{-2}), enthalpy of fusion for infinitely thick crystallite (ΔH: 288.10^6 J m^{-3}) and equilibrium melting temperature (T_m^0: 414.5 K).

Fig. 5a–b show the most important points of the distributions of lamellae thickness calculated with Equation (1). Only samples treated with equal peroxide concentration are compared in each figure. Abscissa denotes crystallite thickness, and ordinate corresponds to area fractions. The common feature to be observed is that the qualitative description suggested earlier for the effects of the peroxide attack is experimentally verified. For each of the samples analyzed, for these peroxide concentrations range the effects consist of simultaneous reduction of the thicker crystallite population and increase of the crystallite population that follows closer at lower crystallite thickness.

4. Conclusions

A calorimetric SSA based technique can be used to study semicrystalline solid structural variations in crosslinked ethylene–butene copolymers. The evolution of crystal size populations with the degree of the peroxide modification process can be explained by considering the increasing concentration of crosslink sites that alter the length and mobility of the methylene chains.

The SSA methodology is proposed as a complementary tool to other characterization techniques suitable of collecting experimental data for modeling verification. However, qualitative information can be gathered using SSA alone to study crosslinking processes. For processes where crosslinking is the predominant reaction, the decrease in SSA peak area fractions will be proportional to the peak area fractions measured for the unmodified polymer. Molecular modeling is needed to quantify the effects observed by SSA.

Acknowledgements

The authors would like to acknowledge the financial support of the National Research Council of Argentina (CONICET), ANPCyT (Project PICT 05-32379) and the Iberoamerican Program CYTED (VIII-11).

References

[1] Krentsel BA, Kissin YV, Kleiner VI, Stotskaya LL. In: Polymers and copolymers of higher α-olefins. chemistry, technology, applications. Munich Hanser Publishers; 1997. p. 299.
[2] Xantos M. Reactive extrusion. New York: Hanser Publishers; 1992.
[3] Paolini Y, Ronca G, Feijoo JL, Da Silva E, Ramirez J, Muller AJ. Macromol Chem Phys 2001;202(9):1539–47.
[4] Bremner T, Rudin A, Haridoss S. Polym Eng Sci 1992;32(14):939–43.
[5] Gloor PE, Tang Y, Kostanska AE, Hamielec AE. Polymer 1994;35(5):1012–30.
[6] Pérez CJ, Cassano GA, Vallés EM, Failla MD, Quinzani LM. Polymer 2002;43(9):2711–20.
[7] Smedberg A, Hjertberg T, Gustafsson B. Polymer 1997;38(16):4127–38.
[8] Nicolás J, Villarreal N, Gobernado I, Merino JC, Pastor JM. Macromol Chem Phys 2003;204(18):2212–21.
[9] Pérez CJ, Vallés EM, Failla MD. Polymer 2005;46(3):725–32.
[10] Andreucetti N, Pérez CJ, Failla M, Vallés E. Macromol Symp 2006;245–246(1):93–105.
[11] Hulse GE, Kersting RJ, Warfel DR. J Polym Sci Polym Chem 1981;19(3):655–67.
[12] Boer J, Pennings AJ. Polymer 1982;23(13):1944–52.
[13] Narkis M, Raiter I, Shkolnik S, Sigmann A. J Macrom Sci Phys 1987;B26:37–58.
[14] Lambert WS, Phillips PJ. Polymer 1990;31(11):2077–82.
[15] Bremner T, Rudin A. J Appl Polym Sci 1993;49(5):785–98.
[16] Lambert WS, Phillips PJ, Lin JS. Polymer 1994;35(9):1809–18.
[17] Sajkiewicz P, Phillips PJ. J Polym Sci Polym Chem 1995;33(6):949–55.
[18] Bremner T, Rudin A. J Appl Polym Sci 1995;57(3):271–86.
[19] Kang TK, Ha CS. Polym Test 2000;19(7):773–83.
[20] Palmlof M, Hjertberg T. Polymer 2000;41(17):6497–505.
[21] Marquez L, Rivero I, Müller AJ. Macromol Chem Phys 1999;200(2):330–7.
[22] Villarreal N, Pastor JM, Perera R, Rosales C, Merino JC. Annual technical conference of the society of plastics engineers. ANTEC. San Francisco: Estados Unidos de América; 2002.
[23] Müller A, Arnal ML. Prog Polym Sci 2005;30(5):559–603.
[24] Morton M, Fetters LJ. Rubber Chem Technol 1975;48:359.
[25] Rachapudy GG, Smith VR, Raju R, Graessley WW. J Polym Sci Polym Phys 1979;17(7):1211–22.
[26] Carella JM, Grassley WW, Fetters LJ. Macromolecules 1984;17(12):2775–86.
[27] Doi Y, Yano A, Soga K, Burfield D. Macromolecules 1986;19(9):2409–12.
[28] Fillon B, Wittmann J, Lotz B, Thierry A. J Polym Sci Polym Phys 1993;31(10):1383–93.
[29] Flory PJ. Principles of polymer chemistry [chapter 9]. New York: Cornell University Press; 1953.
[30] Eliçabe G, Cordon C, Carella JM. J Polym Sci Polym Phys 1996;34(6):1147–54.
[31] Gedde UW. Polymer physics. London: Chapman & Hall; 1995.
[32] Graessley WW, Edwards SF. Polymer 1981;22(10):1329–34.
[33] Abe Y, Flory PJ. Macromolecules 1971;4(2):219–29.
[34] Starck P. Polym Int 1996;40(2):111–22.